

Structural and Kinetic Characterization of Simple Complexes as Models for Vanadate-Protein Interactions

Debbie C. Crans,*† Per Magnus Ehde,‡ Paul K. Shin,† and Lage Pettersson*‡

Contribution from the Department of Chemistry, Colorado State University, Fort Collins, Colorado 80523, and Department of Inorganic Chemistry, Umeå University, S-90187 Umeå, Sweden. Received March 20, 1990

Abstract: The structural and kinetic properties of the complexes that form between vanadate and diethanolamine (DEA) and vanadate and *N*-[tris(hydroxymethyl)methyl]glycine (Tricine) were characterized by use of potentiometry and ^{51}V , ^1H , and ^{13}C NMR spectroscopy. Formation constants were determined in 0.6 M Na(Cl) at 25 °C. The $\text{p}K_{\text{a}}$ values were determined for DEA ($\text{p}K_{\text{HDEA}^+} = 9.072 \pm 0.003$) and Tricine ($\text{p}K_{\text{HTricine}^+} = 2.020 \pm 0.001$, $\text{p}K_{\text{Tricine}} = 7.929 \pm 0.004$). The ternary system $\text{H}^+ - \text{H}_2\text{VO}_4^- - \text{DEA}$ contained one complex with a (0,1,1) composition and a charge of -1 with $\log \beta_{0,1,1} = 3.02 \pm 0.02$. The ternary system $\text{H}^+ - \text{H}_2\text{VO}_4^- - \text{Tricine}$ contained two complexes of the compositions (0,1,1) and (1,1,1), respectively. The (0,1,1) complex had an overall charge of -1, and the (1,1,1) complex was neutral. The $\log \beta_{0,1,1} = 3.65 \pm 0.01$, and the $\log \beta_{1,1,1} = 6.69 \pm 0.07$. The structural characteristics of the V-Tricine (0,1,1) complex were further explored by ^1H and ^{13}C NMR spectroscopy. The Tricine in the V-Tricine complex was found to bind to vanadium through a hydroxyl, the carboxylate, and the amine group. By use of 2D ^{13}C EXSY NMR, the intramolecular exchange rate constant of the three hydroxyl groups in the V-Tricine (0,1,1) complex was measured to be 3.1 s^{-1} at 273 K. Correspondingly, the intermolecular exchange rate constant between Tricine and the (0,1,1) complex was determined to be 5.3 s^{-1} at 298 K. This microscopic rate constant corresponds to a second-order rate constant of $0.76 \times 10^4 \text{ M}^{-1} \text{ s}^{-1}$. These observations combined with previous studies are in accord with the interpretation that the rate of complex formation is limited by the loss of a hydroxo or aqua ligand in the vanadium complexes. The structural preferences and kinetic properties observed for these complexes may aid in understanding the chemical interactions of vanadate with amino acids, peptides, and proteins and the biological activities of vanadium.

Introduction

Vanadium is an important dietary trace element that has many biological activities.¹ It is a required metal for several haloperoxidases and nitrogenases. Vanadates' similarities with inorganic phosphates have resulted in the discovery of many inhibitory effects of vanadate with enzymes including ribonucleases, phosphatases, ATPases, and myosin.¹ The effects of vanadate on enzymes such as glucose-6-phosphate dehydrogenase,^{2a} glycerol-3-phosphate dehydrogenase,^{2b} 6-phosphogluconate dehydrogenase,³ phosphoglucomutase,⁴ phosphoglycerate mutase,⁵ and seminal fluid acid phosphatase⁶ show that the analogy of monomeric vanadate with inorganic phosphate is not the only activity vanadate exhibits. Vanadate has been found to interact with biological molecules through various functionalities including hydroxyl,⁷ carboxylic acid,⁸ phosphate,⁹ and amine groups.^{10,11} Such chemical interactions with proteins and/or other cellular components are likely to be key in understanding the biological effects of vanadium.

The interactions between vanadate and organic ligands in aqueous solution are governed by the versatile coordination chemistry of vanadium(V). Coordination numbers (CN) of organic vanadium compounds reported by X-ray analysis range from 4 to 8. The structure of the vanadium complexes in solution may be different than X-ray structures because of the rapid exchange that occurs between vanadate derivatives and various functionalities present in the particular solutions.^{12,13} Crystals of vanadium(V)-containing compounds obtained from aqueous or mixed aqueous-organic solutions have coordination numbers of 5-7 with ligands including quinolinolate (CN = 5),¹⁴ 2-chloroethanolate (CN = 5),¹⁵ oxalate (CN = 6),¹⁵ EDTA (CN = 6),¹⁶ and citrate (CN = 7).¹⁷ The heptacoordination in the citrate complex is presumably caused by the ligated peroxo group. A coordination number of 5 and a trigonal-bipyramidal structure around the vanadium have been deduced for ethylene glycol, lactate, and glycerate complexes in aqueous solution by use of ^{51}V NMR spectroscopy.^{7,8} An octahedral vanadium was reported for dipeptide complexes of vanadate that were studied with ^{51}V NMR spectroscopy.¹¹ The growing interest in the interaction of vanadium with biological systems increases the need to probe the

stereochemistry of simple vanadate systems in aqueous solutions.

The reaction of vanadate with diethanolamine or related ligands in the neutral pH range generates a 1:1 complex with a chemical shift of -490 ppm.^{10a} This V-DEA complex was previously studied

- (1) (a) Nechay, B. R.; Nanninga, L. B.; Nechay, P. S. E.; Post, R. L.; Grantham, J. J.; Macara, I. G.; Kubena, L. F.; Phillips, T. D.; Nielsen, F. H. *Fed. Proc.* **1986**, *45*, 123-32. (b) Chasteen, N. D. *Struct. Bonding (Berlin)* **1983**, *53*, 105-38. (c) Gresser, M. J.; Tracey, A. S.; Stankiewicz, P. J. *Adv. Protein Phosphatases* **1987**, *4*, 35-57.
- (2) (a) Crans, D. C.; Schelble, S. M. *Biochemistry* **1990**, *29*, 6698-706. (b) Crans, D. C.; Simone, C. M. *Biochemistry* **1991**, in press.
- (3) Crans, D. C.; Willging, E. M.; Butler, S. R. *J. Am. Chem. Soc.* **1990**, *112*, 427-32.
- (4) (a) Layne, P. P.; Najjar, V. A. *Proc. Natl. Acad. Sci. U.S.A.* **1979**, *76*, 5010-3. (b) Percival, P. J.; Doherty, K.; Gresser, M. J. *Biochemistry* **1990**, *29*, 2764-9. (c) Ray, W.; Post, C. B. *Biochemistry* **1990**, *29*, 2779-89.
- (5) Stankiewicz, P. J.; Gresser, M. J.; Tracey, A. S.; Hass, L. F. *Biochemistry* **1987**, *26*, 1264-9.
- (6) Crans, D. C.; Simone, C. M.; Saha, A. K.; Glew, R. H. *Biochem. Biophys. Res. Commun.* **1989**, *165*, 246-50.
- (7) (a) Gresser, M. J.; Tracey, A. S. *J. Am. Chem. Soc.* **1985**, *107*, 4215-20. (b) Gresser, M. J.; Tracey, A. S. *J. Am. Chem. Soc.* **1986**, *108*, 1935-9.
- (8) (a) Tracey, A. S.; Gresser, M. J.; Parkinson, K. M. *Inorg. Chem.* **1987**, *26*, 629-38. (b) Rehder, D.; Priebsch, W.; Oeynhausen, M. von. *Angew. Chem.* **1989**, *101*, 1295-6 (*Angew. Chem., Int. Ed. Engl.* **1989**, *28*, 1221-2).
- (9) (a) Tracey, A. S.; Gresser, M. J.; Parkinson, K. M. *J. Am. Chem. Soc.* **1986**, *108*, 6229-34. (b) Tracey, A. S.; Gresser, M. J.; Galeffi, B. *Inorg. Chem.* **1988**, *27*, 157-61.
- (10) (a) Crans, D. C.; Shin, P. K. *Inorg. Chem.* **1988**, *27*, 1797-1806. (b) Weidemann, C.; Priebsch, W.; Rehder, D. *Chem. Ber.* **1989**, *122*, 235-43.
- (11) Rehder, D. *Inorg. Chem.* **1988**, *27*, 4312-6.
- (12) Recent studies include: (a) Rithner, C. D.; Crans, D. C. 30th Experimental NMR Conference, Asilomar Conference Center, Pacific Grove, California, April 2-6, 1989. (b) Crans, D. C.; Rithner, C. D.; Theisen, L. A. *J. Am. Chem. Soc.* **1990**, *112*, 2901-8. (c) Whittaker, M. P.; Asay, J.; Eyring, E. M. *J. Phys. Chem.* **1966**, *70*, 1005-8. For an overview, see: (d) Pope, M. T. *Heteropoly and Isopoly Oxometalates*; Springer-Verlag: New York, 1983.
- (13) (a) Heath, E.; Howarth, O. W. *J. Chem. Soc., Dalton Trans.* **1981**, 1105-10. (b) Howarth, O. In *Multinuclear NMR*; Mason, J., Ed.; Plenum: New York, 1988; Chapter 5.
- (14) Nakasuka, N.; Tanaka, M. *Acta Crystallogr.* **1989**, *C45*, 1303-6.
- (15) Priebsch, W.; Rehder, D. *Inorg. Chem.* **1990**, *29*, 3013-9.
- (16) (a) Scheidt, W. R.; Tsai, C.-V.; Hoard, J. L. *J. Am. Chem. Soc.* **1971**, *93*, 3867-72. (b) Scheidt, W. R.; Collins, D. M.; Hoard, J. L. *J. Am. Chem. Soc.* **1971**, *93*, 3873-7. (c) Scheidt, W. R.; Countryman, R.; Hoard, J. L. *J. Am. Chem. Soc.* **1971**, *93*, 3878-82.
- (17) Djordjevic, C.; Lee, M.; Sinn, E. *Inorg. Chem.* **1989**, *28*, 719-23.

*Colorado State University.
†Umeå University.

with use of ^{51}V NMR spectroscopy and has been used as a convenient reference compound for biological studies using ^{51}V NMR spectroscopy.^{10a,18} Tridentate ligands containing certain structural functionalities and vanadate generally form stable complexes. These functionalities include a central amino group and two ethylene arms with two hydroxyl groups. The hydroxyl groups on the ethylene arms can be substituted with either carboxylic acids, phosphoric acids, or amines. A pentacoordinate vanadium atom was presumed in the previously studied complexes of monodentate ligands on the basis of ^{51}V NMR spectroscopy.⁷⁻⁹ Recent structural data of a vanadium(V) complex and a somewhat related complex contained pentacoordinated vanadium was reported.^{15,19} This paper describes detailed studies using emf data combined with ^{51}V NMR spectroscopy and computer modeling to characterize the vanadium(V) species in solution. We will use ^1H and ^{13}C NMR spectroscopy to characterize the structural and kinetic properties of amino acid derived ligands complexed to the vanadium.

Most millimolar solutions of vanadate derivatives will contain a minimum of four vanadium species in the physiological pH range. Due to this complexity, very little kinetic data is currently available on formation and hydrolysis of vanadium complexes. The exchange rates of a few complexes (including the V-EDTA complex) have been determined by stopped-flow techniques.^{20,21} Such studies were conducted at low vanadate concentrations because vanadate oligomerizes above 0.1–0.2 mM total vanadate. At such vanadate concentrations, the reaction of EDTA and alizarin (1,2-dihydroxyanthraquinone) with vanadate generated complexes with second-order rate constants of similar magnitude.²⁰ The authors suggested that the rate-limiting step for complex formation was the loss of a hydroxo or aqua ligand.²⁰ If indeed the kinetics of vanadate complex formation with proteins or protein-like ligands was governed by loss of a hydroxo or aqua ligand, such finding would significantly increase the chemist's and biochemist's tools when studying how vanadium interacts in biological systems.^{22,23} We have therefore studied amino acid derived ligands with several functionalities and their complex formation as a model for how amino acids, peptides, and proteins may interact with vanadate in biological systems.

Experimental Section

Reagents. The reagents used in this work were all reagent grade. The water was distilled and further deionized on an anion-exchange column. The water used in the emf studies was furthermore boiled to remove CO_2 and other soluble gases. Vanadium pentoxide was purchased from Fischer Scientific Co., diethanolamine (DEA) was purchased from Eastman Organic Chemicals, and other chemicals were purchased from Aldrich. The reagents were used without further purification. The standard vanadate solution was prepared by dissolving vanadium pentoxide with ~ 2 equiv of sodium hydroxide (or sodium deuterioxide) in deionized and distilled water (or D_2O). Solutions for the emf studies were prepared as reported previously.²⁴

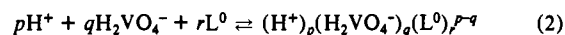
Potentiometric Measurements. A series of potentiometric titrations in 0.6 M NaCl at 25 ± 0.1 °C was performed with use of an automated potentiometric titrator. The concentration of sodium ions ($[\text{Na}^+]$) was kept constant at 0.6 M, and the concentration of chloride ion varied slightly if the solutions had other sources of Na^+ in addition to NaCl (for example, NaH_2VO_4). In most titrations, Ingold 201 NS glass electrodes were used. The glass electrodes were tested against a hydrogen electrode in the alkaline pH range, and accurate measurements were carried out up to $\text{pH} \approx 9.5$. The hydrogen electrode could not be used in the ternary

systems because the vanadium(V) reacted with H_2 . The free hydrogen ion concentration was calculated from the measured emf with the Nernst equation (1) where $g = 59.157$, $j_{\text{ac}} = -76$, $j_{\text{alk}} = 42.5$, and $\log K_w = -13.727$ in 0.6 M NaCl at 25 °C. The j_{ac} and j_{alk} are the liquid

$$E/mV = E_0 + g \log [\text{H}^+] + j_{\text{ac}}[\text{H}^+] + j_{\text{alk}}[\text{H}^+]^{-1}K_w \quad (1)$$

junction potentials and K_w is the ionic product for water. The E_0 was measured in solution with known $[\text{H}^+]$ concentration both before and after each titration.

Terminology. The equilibria are defined by three components, H^+ , H_2VO_4^- , and uncharged ligand, L^0 . The complexes that form can therefore be described according to (2). The complexes were designated



(p, q, r) and the formation constants $\beta_{p,q,r}$. The total concentrations of vanadate, diethanolamine, and Tricine were called V_{tot} , DEA_{tot} , and $\text{Tricine}_{\text{tot}}$, and the protonated, neutral, and deprotonated forms of the ligand were called HL^+ , L^0 , and L^- . The concentration of protons above the zero level of H_2O , H_2VO_4^- , and L^0 is designated H . The deviation between H calculated from potentiometric data, H_{calc} , and H calculated from known total concentrations, H_{tot} , is called ΔH .

Computer Calculations and Modeling. The ternary data were analyzed with use of the least-squares program LAKE,²⁵ which has a (p, q, r) grid facility that simplifies the analysis of experimental data. This procedure first determines the sum of the squared errors, ($U \approx \sum (W_i \Delta A_i)^2$) where ΔA_i is the deviation between A_i calculated from equilibrium constants and total concentrations and A_i calculated from experimental data in each data point. A_i can be either the total concentrations of components, free species concentration, NMR peak integrals, chemical shifts, or combinations of these. W_i is a weighting factor. After the calculation of U ($\approx \sum (W_i \Delta A_i)^2$), a ternary species with its (p, q, r) is added to the fit and the β that gives the lowest U is calculated. The program then proceeds to vary p, q , and r within operator-chosen limits. The set of (p, q, r) that gives the lowest U and/or the lowest error on β is the best fit of data. In the LAKE program, the error on all the total concentrations is minimized; however, we have used a weighting factor that gives ΔH a predominant contribution in the sum of residuals. Thus, when the total concentrations of H^+ (H), vanadate (V_{tot}) and ligand (L_{tot}) are given the weight 1, 100, and 100, respectively, these assumptions make the calculations with the LAKE program equivalent to LETAGROP²⁶ calculations. The distribution of vanadate- or ligand-containing species was plotted with use of the SOLGASWATER program.²⁷ The calculations were carried out with a Cromemco System 300 and a CD Cyber 180-850 at the University of Umeå.

^{51}V -Spectroscopy Methods. The ^{51}V NMR spectra were recorded on a ^1H 200-MHz Bruker WPSY (4.7 T), a ^1H 250-MHz Bruker ACP (5.9 T), or a ^1H 500 MHz Bruker AM (11.7 T) spectrometer. The probe temperature was 24 ± 1 °C. The spectra were obtained from the accumulation of 3000–10 000 transients with use of spectrum widths from 8000 to 20 000 Hz, a 90° pulse angle, an accumulation time of 0.25, and no relaxation delay. No change in the integration of various peaks was observed if the relaxation delay was increased. The chemical shifts are reported relative to the external reference standard VOCl_3 (0 ppm). The ^1H and ^{13}C NMR spectra were recorded on a ^1H 300-MHz Bruker AM spectrometer using the standard parameters. When the ^1H spectra were recorded, a routine for suppressing the HOD signal was employed. The spectra were recorded at various temperatures including 0, 25, and 37 °C.

^{13}C EXSY Spectroscopy.²⁸ The phase-sensitive ^{13}C homonuclear 2D EXSY experiments were done at 75 MHz on a ^1H 300-MHz Bruker AM spectrometer. The spectra were run with temperature control at either 0, 25, or 37 °C. The standard NOESY pulse sequence ($90^\circ-t_1-90^\circ-\tau_m-90^\circ$) supplied with the Bruker software was used to define the experiment. A mixing time of 0.3 s was used. We narrowed the spectral window down to 35 ppm or less to include only the signal region of interest. This reduces the size of the data matrix required in the F_1 domain. A total of 200 accumulations was made for each of 80 t_1 increments.

The 2D ^{13}C spectra gave exchange cross-peaks between selected diagonal signals. Integrations of the peak volumes were carried out by integration of the individual row and column slices of the 2D spectral

(18) Crans, D. C.; Bunch, R. L.; Theisen, L. A. *J. Am. Chem. Soc.* **1989**, *111*, 7597–607.

(19) Diamantis, A. A.; Frederiksen, J. M.; Salam, Md. A.; Snow, M. R.; Tiekink, E. R. T. *Aust. J. Chem.* **1986**, *39*, 1081–8.

(20) Kustin, K.; Toppen, D. L. *J. Am. Chem. Soc.* **1973**, *95*, 3564–8.

(21) Amos, L. W.; Sawyer, D. T. *Inorg. Chem.* **1972**, *11*, 2692–7.

(22) (a) Vilter, H.; Rehder, D. *Inorg. Chim. Acta* **1987**, *136*, L7–L10. (b) Butler, A.; Danzitz, M. J.; Eckert, H. *J. Am. Chem. Soc.* **1987**, *109*, 1864–5. (c) Rehder, D.; Holst, H.; Quaas, R.; Hinrichs, W.; Hahn, U.; Saenger, W. *J. Inorg. Biochem.* **1989**, *37*, 141–50.

(23) Willsky, G. R.; White, D. A.; McCabe, B. C. *J. Biol. Chem.* **1984**, *259*, 13273–81.

(24) Pettersson, L.; Hedman, B.; Andersson, I.; Ingri, N. *Chem. Scr.* **1983**, *22*, 254–64.

(25) (a) Holmström, K. Ph.D. Thesis, Umeå University, 1988. (b) Ya-

gasaki, A.; Andersson, I.; Pettersson, L. *Inorg. Chem.* **1987**, *26*, 3926–33.

(26) Ingri, N.; Sillén, L. G. *Ark. Kemi.* **1964**, *23*, 97–121.

(27) Eriksson, G. *Anal. Chem. Acta* **1979**, *112*, 375–83.

(28) (a) Perrin, C. L.; Gipe, R. K. *J. Am. Chem. Soc.* **1984**, *106*, 4036–8.

(b) Johnston, E. R.; Dellwo, M. J.; Hendrix, J. *J. Magn. Reson.* **1986**, *66*, 399–409.

Table I. Formation Constants for Various Species in the Binary Systems $H^+-H_2VO_4^-$, H^+-DEA^a and $H^+-Tricine^b$ (0.6 M NaCl), 25 °C^c

<i>p, q, r</i>	$\log \beta_{pqr}$	pK_a	formula/abbrev
$H^+-Vanadate^d$			
1, 0, 0			H^+
-1, 1, 0	-7.92		HVO_4^{2-}
0, 1, 0		7.92	$H_2VO_4^-$
-2, 2, 0	-15.2		$V_2O_7^{4-}$
-1, 2, 0	-5.25	9.92	$HV_2O_7^{3-}$
0, 2, 0	2.77	8.02	$H_2V_2O_7^{2-}$
-2, 4, 0	-8.88		$V_4O_{13}^{6-}$
-1, 4, 0	0.22	9.10	$HV_4O_{13}^{5-}$
0, 4, 0	10.00		$V_4O_{12}^{4-}$
0, 5, 0	12.38		$V_5O_{15}^{5-}$
4, 10, 0	52.13		$V_{10}O_{28}^{6-}$
5, 10, 0	53.13	6.00	$HV_{10}O_{28}^{5-}$
6, 10, 0	61.87	3.74	$H_2V_{10}O_{28}^{4-}$
7, 10, 0	63.47	1.6	$H_3V_{10}O_{28}^{3-}$
2, 1, 0	6.96		VO_2^+
H^+-DEA^a			
0, 0, 1			$C_4H_{11}O_2N/DEA$
1, 0, 1	9.072 ± 0.003	9.072	$C_4H_{12}O_2N^+/HDEA^+$
$H^+-Tricine^b$			
-1, 0, 1	-7.929 ± 0.001		$C_6H_{12}O_5N^-/Tricine^-$
0, 0, 1		7.929	$C_6H_{13}O_5N/Tricine$
1, 0, 1	2.020 ± 0.004	2.02	$C_6H_{14}O_5N^+/HTricine^+$

^a DEA = diethanolamine. ^b Tricine = *N*-[tris(hydroxymethyl)-methyl]glycine. ^c The results were obtained by use of the computer program LAKE.²⁵ ^d Results taken from ref 24 and recalculated with $H_2VO_4^-$ as the component in place of HVO_4^{2-} .

matrix with use of standard Bruker software, DISRNMR. The volume elements obtained were normalized by using the relative peak integrals from a 1D ¹³C spectrum. The normalized intensity matrix was diagonalized by an adapted routine from EISPAAC for solving real and general matrices. The exchange matrix calculated in this manner contains specific rate constants for exchange of magnetization between sites.

Detailed description of error analysis for the 2D EXSY experiments has been described previously.²⁹ The errors arise from the limited signal to noise ratios of the computed spectra, instrumental drift during the experiment, or errors in the 2D signal integration. The reproducibility on the calculation of the rate constants was 5%. We estimate that the rate constants are determined with a 20–40% accuracy.

NMR Sample Preparation. The vanadate solutions were prepared by mixing various amounts of vanadate, ligand, and potassium chloride or sodium chloride. The ¹H NMR samples were prepared using standard solutions made up in deuterium oxide. The ¹³C NMR samples contained 20% deuterium oxide.

Results and Discussion

Binary Systems. The binary subsystems in a ternary system ($H^+-H_2VO_4^-L$) must each be accurately known in order to properly characterize speciation. The DEA and Tricine systems were studied from 2.5 to 40 mM DEA_{tot} or $Tricine_{tot}$. By use of 62 titration points (six titrations), the pK_{HDEA^+} was determined to 9.072 ± 0.003 (Table I). By use of 150 titration points (nine titrations), the $pK_{HTricine^+}$ was determined to 2.020 ± 0.004 , and by use of 69 titration points (six titrations), the $pK_{Tricine}$ was determined to 7.929 ± 0.001 (Table I). The vanadate system ($H^+-H_2VO_4^-$) has previously been studied in 0.6 M NaCl) and at 25 °C.²⁴ All the species and formation constants are summarized in Table I.

$H^+-H_2VO_4^-DEA$ System. The reaction of vanadate with DEA can be written in the general terms as (3). The complex shown in (3) is described as complex (*p, q, r*). In agreement with ⁵¹V

$$pH^+ + qH_2VO_4^- + rDEA \rightleftharpoons (H^+)_p(H_2VO_4^-)_q(DEA)_{r-q} \quad (3)$$

NMR spectroscopy, the emf measurements show the presence of only one vanadium–ligand complex having a composition of (0,1,1). The second best fit of the data gave a 19 times larger

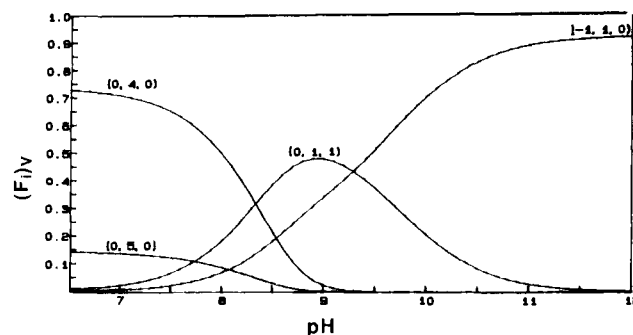
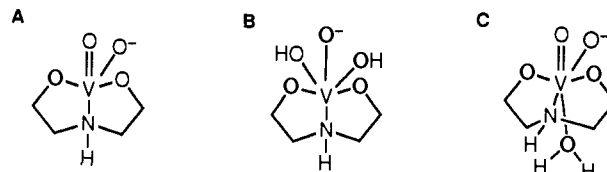


Figure 1. Distribution of vanadium in the ternary system $H^+-H_2VO_4^-DEA$ at 10 mM total vanadate and 40 mM total DEA (0.6 M NaCl), 25 °C) as a function of pH. In the terminology specified in the text, complex (–1,1,0) is HVO_4^{2-} , (0,1,1) is the V–DEA complex, and (0,4,0) is the vanadate tetramer. All species containing less than 1 mM vanadate have been omitted for clarity.

U value and involved the (0,2,2) species in place of the (0,1,1) species. The poor fit of the (0,2,2) species therefore strongly supports the assigned speciation. With use of the emf data, the $\log \beta_{0,1,1}$ was determined to be 3.02 ± 0.02 (Table I). These calculations were based on 73 titration points (nine titrations) from pH 7 to 10, from 5 to 40 mM vanadate, and from 10 to 40 mM DEA with DEA_{tot} to V_{tot} ratios from 1 to 4. The above results agree favorably with previous determinations of $\log \beta_{0,1,1} = 2.7$ in 0.4 M KCl and 0.1 M imidazole at 20 °C.^{10a}

V–DEA Complex: Speciation and pH Dependence. The distribution of vanadium species from pH 6.5 to 12 in a solution containing 10 mM vanadate and 40 mM DEA was calculated and is shown in Figure 1. At pH below 8.5, the vanadate tetramer (0,4,0) is the dominant species; however, as pH increases the contribution of the V–DEA complex becomes more important until it reaches a maximum at pH 9.0. The maximum stability of the V–DEA complex (the highest $[V-DEA]/[V]$ ratio) occurs at $pH = (pK_{H_2VO_4^-} + pK_{HDEA^+})/2 \approx 8.5$ as described previously, although the highest concentration of V–DEA complex is observed slightly above this pH.^{10a} At no point is a (1,1,1) complex observed, and indeed if such a species exist, it must be less than 2% of the total concentration of vanadium atoms in the solution. Monomeric vanadate is monoprotonated (HVO_4^{2-}) and diprotonated ($H_2VO_4^-$) in the pH range from 6 to 9. Since $pK_{H_2VO_4^-}$ is 7.9, the major fraction of the monomeric vanadate below pH 7.9 is $H_2VO_4^-$ and above pH 7.9 it is HVO_4^{2-} . The formation of only one V–DEA complex of a (0,1,1) composition by emf experiments is in agreement with the observations using ⁵¹V NMR spectroscopy.

V–DEA Complex: Structural Considerations. The emf studies yield the stoichiometry of the complex defined by (3) and an overall charge of –1. If the complex contained a pentacoordinate vanadium, one could imagine a structure of the type A. If, on the other hand, the structure contained octahedral vanadium, structures such as B and C would be possible.



Structures A and C are the most likely structures for the V–DEA complex. The difference between structures A and C is the bound water molecule. If one hydrated water molecule is located so close to the vanadium that the O–V distance should be considered a bond, complex C will be the correct structure. If, on the other hand, the O–V distance is very long, complex A is the best description for the complex. The difference between a structure of type A or C is therefore in some sense semantics. We will use the A-type structure for illustrations in this paper since the only structural information on a related structure was found to contain pentacoordinate vanadium.¹⁹

(29) Abel, E. W.; Coston, T. P. J.; Orrell, K. G.; Sik, V.; Stephenson, D. *J. Magn. Reson.* 1986, 70, 34–53.

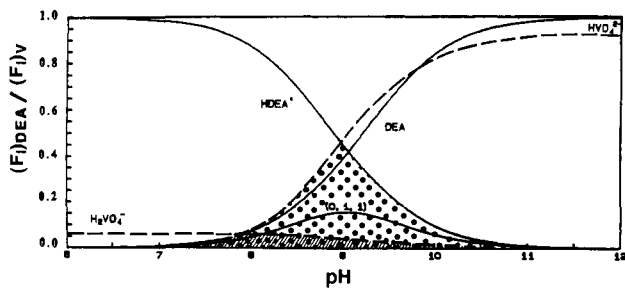
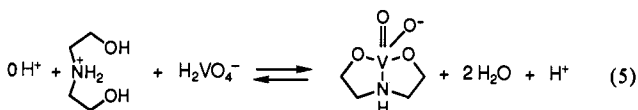
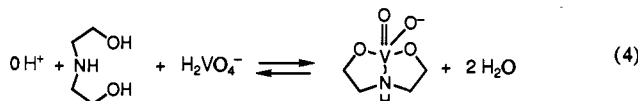
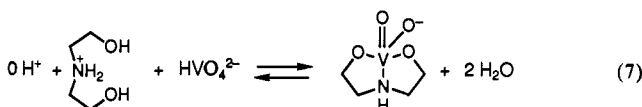
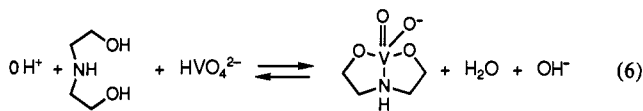


Figure 2. Distribution of DEA in the ternary system $\text{H}^+ - \text{H}_2\text{VO}_4^- - \text{DEA}$ at 10 mM total vanadate and 10 mM total DEA (0.6 M NaCl) at 25 °C as a function of pH. The relative concentrations of H_2VO_4^- and HVO_4^{2-} are shown.

Mechanistic Considerations. Assuming the diprotonated vanadate reacts to form complex A, two possible mechanisms by which this reaction occurs are shown in eqs 4 and 5. The reaction



shown in (4) illustrates the reaction of diprotonated vanadate reacting with neutral ligand (DEA). The reaction shown in (5) illustrates the reaction of diprotonated vanadate with the protonated ligand. Alternatively, monoprotonated vanadate could react with either protonated or neutral ligand to form complex (0,1,1). These possibilities are shown in eqs 6 and 7. We will



focus on reactions 4 and 7 because these two equations directly yield the V-DEA (0,1,1) complex as the product. Reactions 5 and 6 require an additional proton transfer step before the reaction is complete. We will examine the distribution of the ligand and vanadate in the reaction and thus determine the concentration of the species present when the complex is formed.

The stability of the V-DEA (0,1,1) complex as a function of pH and the pH range for DEA and HVO_4^{2-} and their protonated analogues are shown in Figure 2. Reaction 4 occurs when both neutral ligand and diprotonated vanadate are present in solution, and this pH range has been shaded on Figure 2. Reaction 7 occurs when both protonated ligand (HDEA⁺) and monoprotonated vanadate are present in solution, and this pH range has been marked by dots in Figure 2. When reactions occur in vanadate solutions containing many vanadate species in equilibrium with each other, it is not clear which vanadate species kinetically is (are) active in the DEA reaction(s). However, identifying the major species present in the solutions simultaneously with the complex will identify the major species presumably responsible for the thermodynamic stability of the complex. On the basis of these considerations, it is reasonable to expect that the protonated ligand and the monoprotonated vanadate are the major species responsible for the V-DEA complex.

A mechanism for complex formation based on the monoprotonated vanadate and protonated ligand is shown in Scheme I. Although this mechanism is not the only mechanism one can

Scheme I

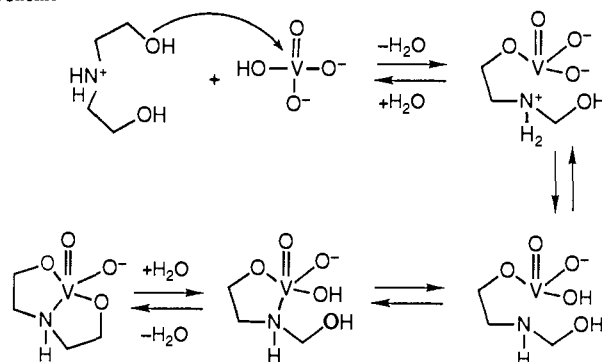


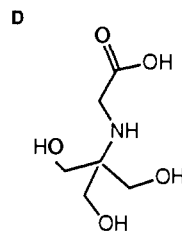
Table II. Formation Constants and ^{51}V Chemical Shift Values for the Ternary Systems $\text{H}^+ - \text{V} - \text{DEA}$ and $\text{H}^+ - \text{H}_2\text{VO}_4^- - \text{Tricine}$ (0.6 M NaCl), 25 °C^a

system	<i>p, q, r</i>	$\log \beta_{pqr} (\pm 3\sigma)$		
		emf	NMR	$\delta (\pm \sigma)$ (ppm)
$\text{H}^+ - \text{V} - \text{DEA}$	0, 1, 1	3.02 (2)	2.7 ^b	-491.1 (2)
$\text{H}^+ - \text{V} - \text{TRI}$	0, 1, 1	3.74 (2)	3.65 (1)	-508.0 (2)
	1, 1, 1	6.70 (6)	6.69 (7)	

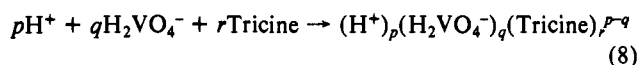
^aThe calculations were carried out with use of the computer programs LETAGROP²⁶ (emf) and LAKE²⁵ (peak integrals). ^bThis formation constant was determined in 0.4 M KCl and 0.1 M imidazole at 20 °C.^{10a}

suggest, it does illustrate the likelihood of several intermediates between the reactants and products. ^{51}V NMR spectra at high DEA concentrations indeed give evidence for formation of the first of these intermediates in rapid exchange with monomeric vanadate.¹⁰ The emf studies, on the other hand, give no evidence for significant concentrations of complexes other than a (0,1,1) complex between vanadate and DEA. However, since all the intermediates shown in Scheme I would be complexes designated as (0,1,1), the intermediates suggested in Scheme I would not be distinguished from the final V-DEA complex by emf titrations.

In order to characterize the properties of vanadium(V) complexes further, we examined the reaction of vanadate with a ligand that had additional structural possibilities for complex formation. This ligand was chosen such that it contained both a carboxylic acid group and a hydroxyl group and that comparisons of these two functionalities could be made. In addition, the ligand contained other functional groups that may form alternative complexes. The chosen ligand should preferably generate a sufficiently stable vanadium complex such that both structural and kinetic studies could be carried out. Last, the ligand should be of sufficient biological interest, preferably an amino acid derivative, that the information obtained in these studies could be used in the interpretation of the interactions of vanadium in biological systems. The ligand we found appropriate for detailed study was a glycine derivative, *N*-[tris(hydroxymethyl)methyl]glycine (Tricine, D).



$\text{H}^+ - \text{H}_2\text{VO}_4^- - \text{Tricine}$ System. The reaction of vanadate with Tricine can be written in general terms as (8). The calculations



on the emf data show the presence of two complexes with the compositions (0,1,1) and (1,1,1) (Table II). These calculations were based on 105 titration points (16 titrations) from pH 1.5

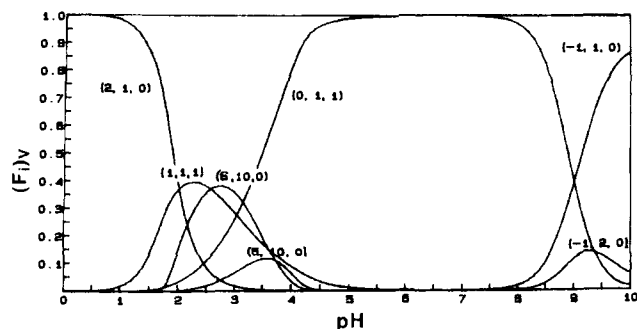
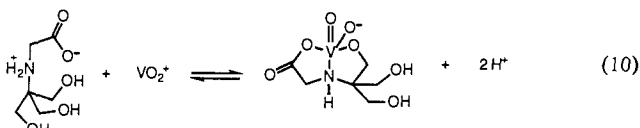
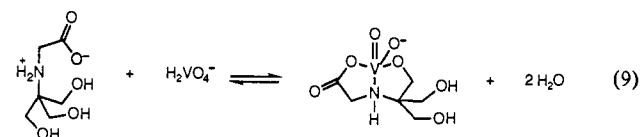


Figure 3. Distribution of Tricine in the ternary system H^+ – H_2VO_4^- –Tricine at 10 mM total vanadate and 40 mM total Tricine (0.6 M NaCl), 25 °C) as a function of pH. The two V–Tricine complexes are designated (0,1,1) and (1,1,1) as described in the text. All species containing less than 1 mM vanadate have been omitted for clarity.

to 8.5, from 5 to 40 mM vanadate, from 2.5 to 40 mM Tricine, and from 0.125 to 8 Tricine_{tot} to V_{tot} ratios. Due to spontaneous reduction of V(V) at acidic pH, rapid titrations of neutral V–Tricine solutions with HCl were carried out in order to obtain the acidic titration points. ^{51}V NMR data (17 spectra; 132 peak integrals) were used to confirm and expand the speciation data to $1.0 < \text{pH} < 9.6$. In the acidic pH range, additional ^{51}V NMR resonances were visible; however, these species amounted to less than 1% total vanadium in the spectra used for our calculations. Calculations based on the emf/NMR data gave a $\log \beta_{0,1,1} = 3.74 \pm 0.02/3.65 \pm 0.01$ and $\log \beta_{1,1,1} = 6.70 \pm 0.06/6.69 \pm 0.07$.

V–Tricine Complexes: Speciation and pH Dependence. The distribution of vanadium as a function of pH has been calculated for Tricine_{tot} = 40 mM and V_{tot} = 10 mM and plotted in Figure 3. The (0,1,1) complex is predominant, and from pH 4.5 to 8 essentially all vanadium is bound in this complex. Below pH 5, the second V–Tricine complex with the composition (1,1,1) emerges. The (1,1,1) complex is not very predominant. It has its maximum concentration at $\text{pH} \approx 2.3$ where it binds $\sim 40\%$ of V_{tot}. At lower pH, the (2,1,0) complex corresponding to VO_2^+ becomes the major vanadium species.

The VO_2^+ and the two decamer complexes are the major vanadium species present in solution in the pH range where the V–Tricine (1,1,1) complex is observed. It is therefore possible that the major species responsible for formation of the V–Tricine (1,1,1) complex are the protonated ligand and VO_2^+ . The major species responsible for formation of the V–Tricine (0,1,1) complex may be the neutral Tricine (zwitterion) and either H_2VO_4^- or VO_2^+ (Figure 4). The reactions generating the V–Tricine (0,1,1) complex are illustrated in eqs 9 and 10. Both (9) and (10) express reactions that seem appropriate when considered in the proper pH range, and both reactions lead to complexes of the (0,1,1) type.



V–Tricine Complex: Structural Studies. The major complex formed from vanadate and Tricine ((0,1,1)) is a 1:1 ligand–vanadium complex with an overall charge of -1 . Complex E is the most likely structure for this (0,1,1) complex if vanadium is pentacoordinate. An alternative pentacoordinate complex is shown as complex F. It is not obvious what would be the best moiety for the H^+ in the complex: the carboxylate, the $-\text{O}-$, or the hydroxyl bound to vanadium. The latter structure does not seem favorable, and as we will discuss in the following text, NMR data

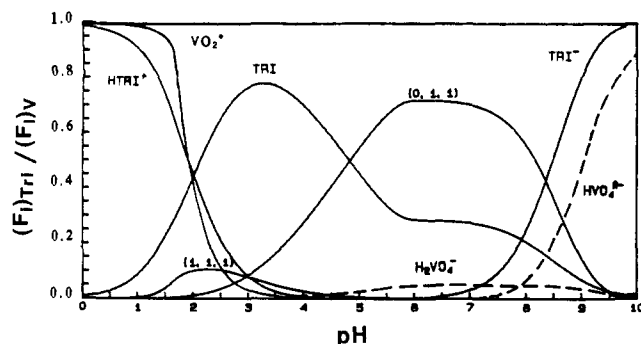
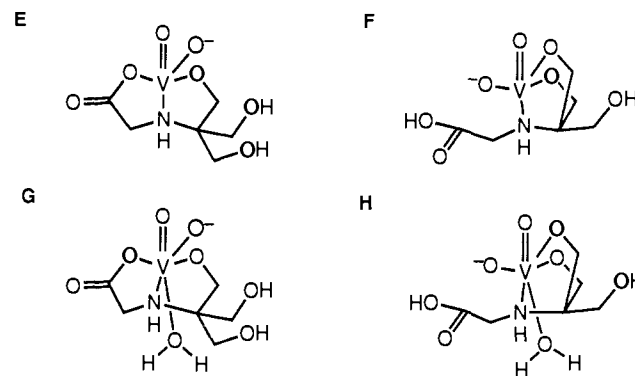


Figure 4. Distribution of Tricine in the ternary system H^+ – H_2VO_4^- –Tricine at 10 mM total vanadate and 10 mM total Tricine (0.6 M NaCl), 25 °C) as a function of pH. The relative concentrations of H_2VO_4^- , HVO_4^{2-} , and VO_2^+ are shown.

indeed suggest that structure E is the structure found in solution. Alternatively, the complex could have an octahedral vanadium atom, and consequently, the analogous structures would be G and H.

^{51}V NMR spectroscopy shows that the V–Tricine is a complex at ~ 508 ppm. As the pH varies from 1 to 9, no changes in the chemical shift are observed. The emf studies show a (1,1,1) complex forms at low pH in a manner that the ^{51}V chemical shift will not be affected. This observation suggests that protonation of the (0,1,1) complex occurs at low pH. We have used ^1H and ^{13}C spectroscopy to further probe the structure of the V–Tricine (0,1,1) complex. Complexes E and F are likely to give different

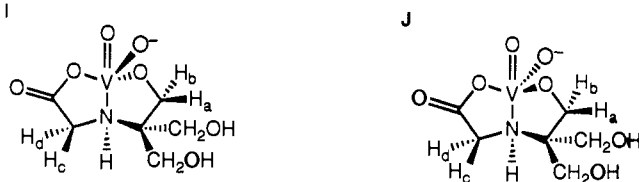


^1H and ^{13}C spectra, and thus, recording these spectra will allow us to distinguish between these complexes. A solution of 412 mM vanadate and 500 mM Tricine at pH 7.1 gives a ^{51}V NMR spectrum that indicates 398 mM vanadate is in the form of the (0,1,1) complex at 25 °C. The ^1H NMR spectrum (also at 25 °C) gives two broad signals at 4.05 and 4.25 ppm, two broad signals at 3.4 and 3.75 ppm, and several other signals from 3.5 to 3.7 ppm. However, when the solution is cooled to 0 °C, an AB pattern appears centered about 4.0 ppm and two sharp singlets presumably accounting for a $-\text{CH}_2-$ group appear at 3.6 and 3.3 ppm. The ^1H spectrum also shows several superimposed signals in the chemical shift range from 3.4 to 3.6 ppm. A ^{13}C NMR spectrum was recorded to help identify the superimposed signals in the ^1H spectrum. Two carboxylic acid signals at 186 and 175 ppm were identified in the ^{13}C spectrum. The carboxylic acid group at 186 ppm is assigned to the complex (large peak), whereas the carboxylic acid at 174 ppm is assigned to the ligand (small peak). This assignment was confirmed by recording a ^{13}C NMR spectrum of the ligand under similar conditions (174, 68, 62, and 46 ppm). The signals observed at 186, 80, 70, 65, 63, and 49 ppm are assigned to the complex. Since the carboxylic acid group in the complex appears at 12 ppm higher frequency than the ligand, the carboxylic acid group in the complex is most likely covalently attached to the vanadium atom. One of the three $-\text{CH}_2\text{O}-$ groups was also found to give a signal at significantly higher frequency (80 ppm) compared to the two other $-\text{CH}_2\text{O}-$ groups (65 and 63 ppm) in the complex. The quaternary carbon in the complex (70

ppm) was found to have a signal 2 ppm higher than the ligand (68 ppm). The $-\text{CH}_2-$ group (49 ppm) adjacent to the carboxylic acid had a signal 3 ppm higher than the ligand (46 ppm). The slight shifts in the chemical shift indicate both the $-\text{CH}_2-$ group and the quaternary carbon are adjacent to a group directly attached to the vanadium atom (that is, a $-\text{CH}_2\text{OV}$ or a $-\text{CH}_2\text{NV}$).

By use of the previous assignments in the ^{13}C NMR spectrum, a HETCOR spectrum was recorded at 0°C to assign the peaks in the ^1H NMR spectrum. The AB pattern in the ^1H NMR spectrum centered about 4.0 ppm correlates with the ^{13}C signal at 80 ppm. These signals are assigned to the $-\text{CH}_2\text{O}-$ group that is covalently attached to the vanadium atom. The two ^1H singlets at 3.6 and 3.3 ppm correlate to the ^{13}C signals at 65 and 63 ppm and are assigned to the two $-\text{CH}_2\text{OH}$ groups in the complex that are not attached to the vanadium. The HETCOR spectrum furthermore reveals an additional AB pattern in the ^1H spectrum correlating with the resonance at 49 ppm in the ^{13}C NMR. These signals are assigned to the $-\text{CH}_2-$ group adjacent to the carboxylate that is directly attached to the vanadium atom. Correspondingly, the signals for the ligand were observed at 3.5 and 3.4 ppm in the ^1H NMR spectrum and correlated with the signals at 61 and 46 ppm in the ^{13}C NMR spectrum. The former signal is assigned to the $-\text{CH}_2\text{OH}$ group in the ligand, and the latter signal (46 ppm) is assigned to the $-\text{CH}_2-$ group adjacent to the carboxylic acid group.

These considerations therefore support a complex in which one $-\text{CH}_2\text{OH}$ group and the $-\text{COO}^-$ group in the ligand are attached to the vanadium in the complex. Complex E fulfills these structural requirements. The fact that two AB patterns have been observed in the ^1H spectrum suggests the V-Tricine complex contains groups that are prochiral; namely, two $-\text{CH}_2\text{OH}$ groups and the $-\text{CH}_2\text{COO}^-$ group. The two free $-\text{CH}_2\text{OH}$ groups in the complex give different signals in both the ^1H and ^{13}C spectrum, supporting the prochiral nature of the complex. As shown by structures I and J, complex E may have either the NH bond trans to the $\text{V}-\text{O}^-$ bond (I) or the NH bond cis to the $\text{V}-\text{O}^-$ bond (J). Since we have no experimental evidence to distinguish these structures, we will refer to complex E in the remainder of this paper.

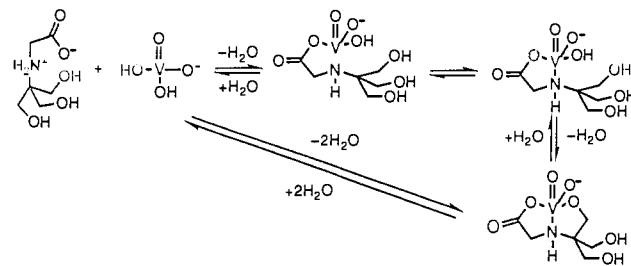


The structure of complex E is of particular interest because it may provide information on the structures of complexes formed between vanadate and proteins. The combination of a carboxylic acid group, a secondary amine, and a hydroxyl group in Tricine appears to yield a favorable geometry that gives this complex its particularly high stability. Substituting either of these groups yields a complex of much lower stability.^{10a} Since complex E contains three different ligand functionalities, several mechanistic possibilities for formation of complex exist, and this complex can be used to probe selectivity and rates of complex formation between various functionalities.

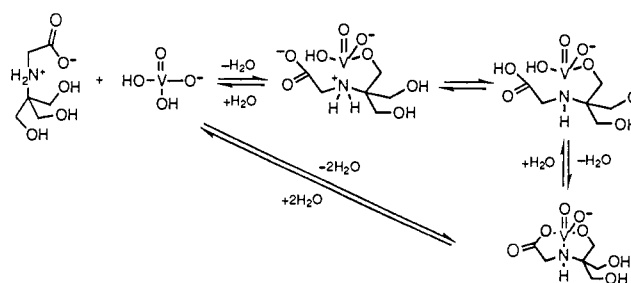
V-Tricine Complex: Kinetics. The two major vanadium species presumably responsible for the stability of the V-Tricine complex are the Tricine zwitterion and H_2VO_4^- . Two reasonable mechanisms for formation of (0,1,1) complex are shown in Schemes II and III. Scheme II illustrates a mechanism in which the attack of the carboxylate is the first reaction step. Scheme III illustrates a mechanism in which the hydroxyl groups attack the vanadium as the first reaction step.

The ^1H spectrum of the complex shows significant line broadening, and a decrease in temperature to 0°C significantly sharpens the signals. It is therefore possible that intramolecular ligand-complex exchange can be determined by use of NMR spectroscopy. The ^1H spectra of the complex-ligand mixture at various temperatures show approached coalescence (Figure 5).

Scheme II



Scheme III



Conducting 2D NMR experiments at elevated temperatures should indeed allow measurement of the intermolecular exchange between ligand and complex. However, as seen in Figure 5, the ^1H spectrum is very complex with several overlapping resonances. Conducting a kinetic analysis using the ^{13}C NMR spectrum should therefore simplify the analysis of both the intra- and intermolecular exchange reaction.

A 2D ^{13}C EXSY experiment was therefore conducted at 25 and 37°C on the sample containing 412 mM vanadate and 500 mM Tricine at 25°C . Such solutions will contain 14 mM vanadate anions, 398 mM complex, and 102 mM free ligand. The ligand and complex signals are therefore readily identified on the basis of intensity. The 2D ^{13}C spectrum recorded at 37°C (Figure 6) shows exchange between the complex and the ligand. The ternary carbon in the complex (C_3) exchanges with the ternary carbon in the ligand (L_3). Furthermore, the $-\text{CH}_2-$ group adjacent to the carboxylic acid group in the complex (C_2) exchanges with the corresponding $-\text{CH}_2-$ in the ligand (L_2). The rate of exchange was calculated with use of the DISRNMR subroutine. Calculations were conducted for the measurement at both 25 and 37°C , but only the rates for the former are reported here. The calculations yielded a microscopic exchange rate constant of 5.3 s^{-1} for the C_2 - L_2 exchange and a microscopic rate constant of 5.2 s^{-1} for the C_3 - L_3 exchange (Table III). These rate constants are sufficiently similar to be identical within experimental uncertainty. This is in accord with the expectation that the exchange rate between the free ligand and ligand in the complex should be the same whether this rate is measured at C_2 or C_3 . Since only vanadate, free ligand, and the V-Tricine (0,1,1) complex are observed in significant concentrations in the NMR spectra, the observed exchange rates are indeed an expression for the intermolecular exchange rate between these species. The microscopic rate constant was measured at 102 mM free Tricine and 0.70 mM monomeric vanadate. If the complex is formed according to (9) or (10) and both monomeric vanadate and Tricine may contribute to the rate-limiting step, the rate of complex formation could be expressed as a second-order reaction (11). Such rate law was

$$\text{rate} = k_f[\text{Tricine}][\text{V}_1] = k_{c \rightarrow L}[\text{Tricine}] \quad (11)$$

$$k_f = k_{c \rightarrow L}/[\text{V}_1] \quad (12)$$

previously found to be the major pathway for complex formation with EDTA and alizarin.²⁰ It is therefore possible to calculate such a second-order rate constant, k_f . On the basis of $k_{c \rightarrow L_2}$ and $k_{c_3 \rightarrow L_3}$, k_f is calculated to $0.76 \times 10^4\text{ M}^{-1}\text{ s}^{-1}$ and $0.75 \times 10^4\text{ M}^{-1}\text{ s}^{-1}$ (Table III).

Exchange was also indicated between C_4 , C_5 , C_6 , and L_4 ; however, the resolution was too poor and/or the intensity too low

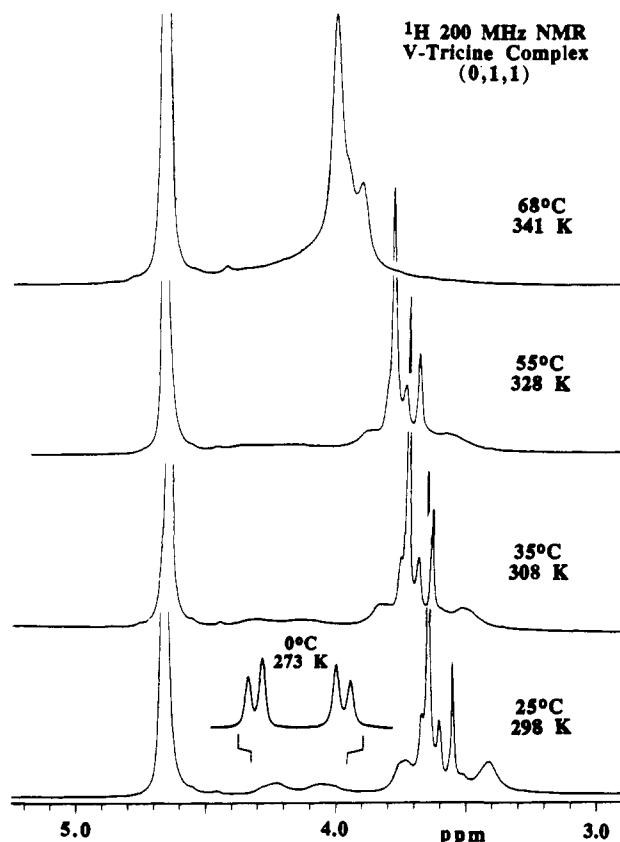


Figure 5. ^1H NMR spectra recorded of a solution containing 412 mM total vanadate and 500 mM total Tricine at pH 7.33. This solution contains 398 mM V-Tricine (0,1,1) complex and 0.61 mM vanadate monomer as determined by ^{51}V NMR spectroscopy at 25 °C and 102 mM free Tricine. The spectra were recorded at 200 MHz at various temperatures.

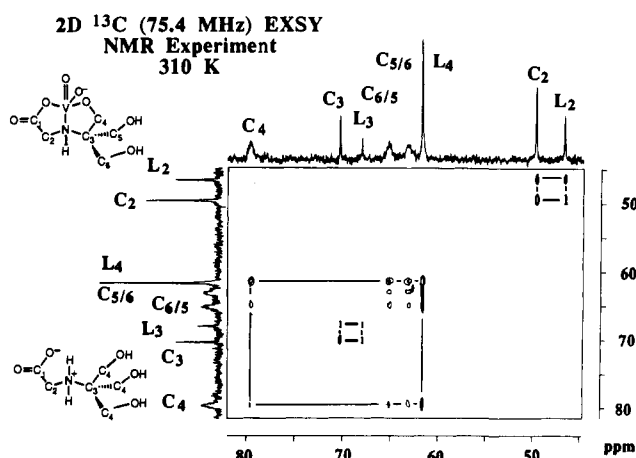


Figure 6. 2D ^{13}C EXSY NMR spectrum recorded at 75.4 MHz (7.05 T) at 37 °C (310 K) of a solution containing 412 mM total vanadate and 500 mM total Tricine at pH 7.2. This solution contains 398 mM V-Tricine (0,1,1) complex and 1.2 mM monomeric vanadate as determined by ^{51}V NMR spectroscopy and 102 mM free Tricine. The microscopic exchange rates were determined from the integrations of a spectrum analogous to this recorded at 25 °C and are shown in Table III.

to yield usable exchange rate constants for these groups.

The rates of formation of a few vanadium(V) complexes have been determined previously with use of several techniques (Table IV). The rate of V-EDTA complex formation was determined by use of stopped flow at 0.32 mM vanadate and 20 mM EDTA and 25 °C. The second order rate constants were determined from 2.34×10^4 to $2.4 \times 10^3 \text{ M}^{-1} \text{ s}^{-1}$ mainly depending on which protonated form of the vanadate species was involved in the reaction.²⁰ The rate constant based on the reaction between H_2VO_4^-

Table III. Exchange Rates and Activation Barriers for the Inter- and Intramolecular Exchange Reaction for the Formation of the V-Tricine (0, 1, 1) Complex

exch mech	ΔG^\ddagger (kcal/mol)	calcd ^a exch rate	exch ^{b,d} rate
	298 K	const (s ⁻¹) 298 K	const (s ⁻¹) 273 K
$\text{C}_2 \leftrightarrow \text{L}_2^a$	16.5	5.3	
$\text{C}_3 \leftrightarrow \text{L}_3^a$	16.5	5.2	
$\text{C}_4 \leftrightarrow \text{C}_{5/6}^b$	15.3	36	3.1
$\text{C}_4 \leftrightarrow \text{C}_{6/5}^b$	15.3	36	3.1
$\text{C}_5 \leftrightarrow \text{C}_6^b$	15.5	28	2.3

^a Inter-molecular exchange mechanism. ^b Intra-molecular exchange mechanism. ^c ΔG^\ddagger is calculated with the following: $\Delta G^\ddagger = -RT \ln(k_{c \rightarrow L}/T)$. Since the rate constants are pseudo-first-order rate constants (see *d*), the calculated ΔG^\ddagger is dependent on experimental conditions. ^d The exchange rates were measured in a solution containing 500 mM total Tricine, 398 mM V-Tricine (0, 1, 1) complex, and 0.70 mM uncomplexed monomeric vanadate. ^e The exchange rate constants at 25 °C (298 K) were calculated with use of the Eyring equation: $k_{c \rightarrow L2} = k_{c \rightarrow L1} T_2/T_1 \exp(\Delta G^\ddagger/R(1/T_1 - 1/T_2))$.

Table IV. Second-Order Rate Constants for Vanadate Complex Formation

ligand	complex	rate constant (M ⁻¹ s ⁻¹)	temp (°C)	ref
vanadate monomer	$\text{H}_2\text{VO}_4^- - \text{HVO}_4^{2-}$ ($\text{HV}_2\text{O}_7^{3-}$)	3.1×10^4	25	12c
		2×10^4	25	12b
alizarin (H ₂ A)	$\text{H}_2\text{VO}_4^- - \text{HA}$	2.8×10^4	25	20
Tricine	$\text{H}_2\text{VO}_4^- - \text{Tricine}$ (0, 1, 1)	0.76×10^4	25	this work
EDTA	$\text{H}_2\text{VO}_4^- - \text{H}_2\text{EDTA}^{2-}$	3.2×10^4	25	20
Na,K-ATPase	$\text{H}_2\text{VO}_4^- - \text{ATPase}$	5.2×10^4	37	30
		$2.9 \times 10^4^a$	25	estimated ^a

^a The rate constant at 25 °C (298 K) was calculated with use of the equation $k_2 = k_1 T_2/T_1 \exp(\Delta G^\ddagger/R(1/T_1 - 1/T_2))$.

and EDTA²⁻ was $2.34 \times 10^4 \text{ M}^{-1} \text{ s}^{-1}$. EDTA is presumably a tetradentate ligand in this complex. A second-order rate term involving H_2VO_4^- and HA^- was also the major reaction path of complex formation between vanadate and alizarin. Alizarin is presumably a bidentate ligand in this complex. This rate constant was $2.28 \times 10^4 \text{ M}^{-1} \text{ s}^{-1}$.²⁰ The vanadate monomer dimerizes with a rate constant of $3.1 \times 10^4 \text{ M}^{-1} \text{ s}^{-1}$ as determined by temperature jump relaxation times^{12c} and estimated to $2 \times 10^4 \text{ M}^{-1} \text{ s}^{-1}$ by 2D ^{51}V EXSY NMR spectroscopy.^{12b} The rate constant for the vanadate interaction with Na,K-ATPase was determined to be $5.2 \times 10^4 \text{ M}^{-1} \text{ s}^{-1}$.³⁰ These measurements were determined from relaxation rates to steady-state turnover at 37 °C.

The rate of the V-Tricine (0,1,1) complex formation at pH 7.2 measured in this paper is presumably expressed by the second-order rate term involving Tricine and H_2VO_4^- . Since the monomeric vanadium species in the pH range of the complex is H_2VO_4^- or VO_2^+ , either species is the $[\text{V}_1]$ used in (11) and (12) and $[\text{Tricine}]$ is the concentration of the zwitterion. The rate constant at 25 °C is calculated to be $0.76 \times 10^4 \text{ M}^{-1} \text{ s}^{-1}$. Tricine is presumably a tridentate ligand in this complex. Normalizing all these rate constants to a common temperature (25 °C) allows direct comparison (Table IV), and all the rate constants are of a similar magnitude.

Vanadate monomer, alizarin, Tricine, EDTA, and Na,K-ATPase form vanadate complexes with similar rate constants (Table IV). These ligands show a considerable spread of basicities. This observation suggests that the rate-limiting step is not effected by the nature of the ligand. It can therefore be concluded that the complexes are not formed by an associative pathway governed by rate-limiting attack by ligand. The examined complexes contain mono, bi, tri, tetra, and polydentate ligands. It therefore appears that the rate-limiting step is not affected by the number of hydroxo, aqua, or other ligands that the vanadium must lose for complex

(30) Cantley, L. C.; Josephson, L.; Gelles, J.; Cantley, L. G. In *Na, K-ATPase Structure and Kinetics*; Skou, J. C., Nørby, J. G., Eds.; 1979; pp 181-91.

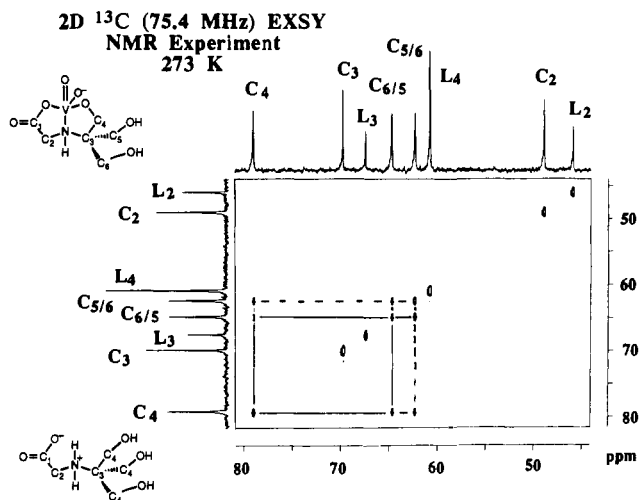


Figure 7. 2D ^{13}C EXSY NMR spectrum recorded at 75.4 MHz (7.05 T) at 0 °C (273 K) of a solution containing 412 mM total vanadate and 500 mM total Tricine at pH 7.1. This solution contains 406 mM V-Tricine (0,1,1) complex and 0.38 mM monomeric vanadate as determined by ^{51}V NMR spectroscopy and 94 mM free Tricine. The microscopic exchange rates were determined from the integrations of these spectra and are shown in Table III.

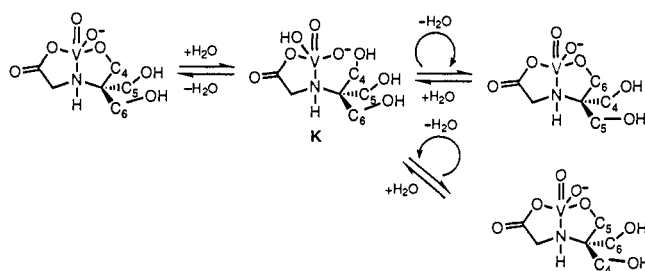
formation. These observations suggest that the loss of the first hydroxo or aqua ligand may be rate-limiting. Previous studies of ligand exchange on vanadium(III), vanadium(IV), vanadium(V), and some oxometallate anions suggest associative types of mechanisms.³¹ Our studies in combination with the results in the literature are of significant interest because they present evidence in favor of a dissociative mechanism. The implication of these findings for the coordination of H_2VO_4^- is of interest although not entirely understood at the present time. If H_2VO_4^- is tetracoordinated, loss of H_2O or OH^- will yield tricoordinated vanadate. Alternatively, a rapid attack of H_2O on H_2VO_4^- would make the vanadium five- or six-coordinated, which could slowly lose a water molecule and leave an open site for an incoming ligand. Precedence for either suggestion has been reported, and further experimental evidence such as MCD studies is needed on this question.³² Since most oxometallate anions form complexes under associative control, our observations are unusual and thus need further examination.

If indeed the reaction was governed by an early dissociative rate-limiting step, it should be possible to explore intramolecular exchange that occurs later in the reaction path in vanadium(V) complexes of multidentate ligands. Since the V-Tricine (0,1,1) complex contains three types of functionalities bound to the vanadium atom, this complex is ideal for 2D EXSY ^{13}C NMR studies.

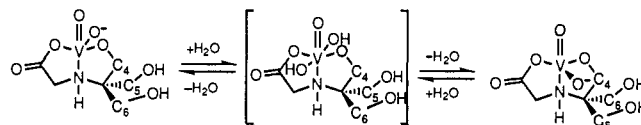
The ^1H NMR spectrum at 0 °C showed increased detail compared to the ^1H NMR spectrum at higher temperatures and may therefore have frozen out possible intramolecular exchange. We therefore conducted a 2D ^{13}C EXSY experiment at 0 °C. The resulting 2D ^{13}C EXSY spectrum shown in Figure 7 indeed shows no intermolecular exchange and neither C_3 and L_3 , C_2 and L_2 , nor C_4 and L_4 are exchanging. The intermolecular exchange between ligand and complex is too slow to be observed under these conditions. However, C_4 exchanges with both C_5 and C_6 , and C_5 exchanges with C_6 . The exchange observed at 0 °C is therefore exclusively intramolecular.

The exchange of C_4 with C_5 or C_6 presumably occurs through a mechanism in which the hydroxyl group arm comes off, there is a rotation around the C-N bond, and the next hydroxyl group binds to the vanadium (Scheme IV). The exchange between C_4 and C_5 occurs if such rotation is clockwise, and the exchange

Scheme IV



Scheme V



between C_4 and C_6 occurs if such rotation is counterclockwise. The mechanism we have shown as Scheme IV shows the addition of water to complex E to form the intermediate K. We have no evidence for this structure, and tetracoordinated or octahedral vanadium are reasonable alternative structures for such intermediates. It is possible that indeed the rate of C_4/C_5 or C_4/C_6 exchange is a measure for the attack of water on vanadium followed by proton transfer to the oxygen on C_4 . The calculations yielded exchange rate constants to be 3.1 s^{-1} (C_4/C_6) and 3.1 s^{-1} (C_4/C_5) (Table III).

A mechanism for direct intramolecular exchange of the C_5 and C_6 groups is shown in Scheme V. There are two plausible mechanisms by which C_5 can exchange with C_6 . The exchange of the C_5 with C_6 can occur through dissociation of the nitrogen followed by inversion on the nitrogen and reattachment to the vanadium. Alternatively, the dissociation of the nitrogen can be followed by rotation with respect to the vanadium group and reattachment of the nitrogen to generate the complex. Dissociation of the nitrogen in the complex represents a reaction path that would increase strain in the complex. Since bidentate ligands with more than a $-\text{CH}_2\text{CH}_2-$ linking group do not seem to form cyclic intermediates, we expect such intermediates are unfavorable. Direct attack of H_2O or OH^- on vanadium followed by proton transfer and dissociation of the other hydroxyl group (that became an aqua group) (Scheme V) represents a more plausible mechanism. It is therefore possible the exchange rate constant of C_5 going into C_6 is an expression for the rate of H_2O or OH^- exchange in the complex. The rate-limiting step of a H_2O exchange reaction could be either the attack or the loss of H_2O . Since complex formation shows little change in rate constants although the ligands vary significantly, it is most likely that the loss of H_2O is the rate-limiting step. The calculations yielded an exchange rate constant for the C_5/C_6 exchange of 2.3 s^{-1} . This rate is very similar to the rate observed for the exchange between C_4/C_5 and C_4/C_6 . It is therefore possible these exchange mechanisms are proceeding through similar reaction steps.

We observe intramolecular exchange of hydroxyl groups and no intramolecular exchange of the carboxylate group. These observations suggest the former is faster than the latter. All the rate constants are normalized to 25 °C (Table III) using the Eyring equation. The results show that the microscopic intermolecular reaction rate is about seven times slower than the microscopic intramolecular reaction rate. The intramolecular microscopic rate constant is a measure for the hydroxyl group exchange in the complex. The intermolecular microscopic rate constant is a measure for reaction between ligand and vanadate. The slow step presumably involves loss of hydroxo or aqua ligands and is followed by attack of the carboxylate on vanadate (see the following text). Comparison of these two microscopic rate constants shows that hydroxyl groups exchange seven times faster than the carboxylate group in Tricine. If the rate-limiting step occurs early on the reaction path and the carboxylate reaction is slow, the attack of the carboxylate group on the vanadium is

(31) Boyd, D. W.; Kustin, K. *Adv. Inorg. Biochem.* 1984, 6, 311-65.

(32) Crans, D. C.; Harnung, S. E.; Larsen, E.; Shin, P. K.; Theisen, L. A.; Trabjerg, I. *Acta Chem. Scand.*, in press.

presumably the first step in complex formation (Scheme II).

Exchange may be controlled by loss of a water molecule analogous to the observations of vanadyl protein complexes.³³ Simple complexes formed from vanadyl cation (VO_2^{2+}) and ligand are kinetically governed by the loss of a water molecule from the first coordination sphere of the hydrated vanadyl cation. In aqueous solutions, the axial water molecule exchanges rapidly ($k \approx 10^8 \text{ s}^{-1}$), whereas the equatorial water molecules are exchanging slower ($k \approx 10^3 \text{ s}^{-1}$).^{33a} In contrast, the vanadyl oxygen is exchanging exceedingly slowly ($k_{\text{ex}} = 3 \times 10^{-5} \text{ s}^{-1}$).^{33b} The exchange between VO_2^{2+} and water in acidic solutions has been determined ($k > 6 \times 10^4 \text{ s}^{-1}$) and found to be faster than exchange of equatorial H_2O at VO_2^{2+} .³⁴ This observation was explained by electrostatic effects on the bonding to the remaining water molecules; namely, the additional oxo ligand compensates for the higher charge on the central metal atom. In the case of vanadate, the exchanging group is an OH^- or O^{2-} and such exchange requires several proton-transfer steps before the actual ligand exchange occurs. Direct comparison between complex formation in acidic and neutral solutions may therefore not be appropriate. It is, however, of interest that complex formation between vanadate and several catechol derivatives lies within the narrow range $1\text{--}10 \times 10^4 \text{ M}^{-1} \text{ s}^{-1}$.³⁴

Conclusions

We have used emf studies and ^1H , ^{13}C , and ^{51}V NMR spectroscopy to examine structural and kinetic properties of vanadium(V) complexes in aqueous solution. Emf and ^{51}V NMR studies have shown that the vanadate–diethanolamine (V–DEA) complex is a 1:1 complex with an overall charge of -1 . The most likely structures for such complexes would have pentacoordinate or octahedral vanadium. We have used pentacoordinate vanadium for illustrations in this manuscript but presently have no experimental evidence to exclude complexes containing octahedral vanadium. DEA is likely to be coordinated to the vanadium through both hydroxyl groups and the amine group. The major species present in solution with the complex, and therefore key species for determining the stability of the V–DEA complex, are HDEA^+ and HVO_4^{2-} . The bell-shaped pH stability curve of the V–DEA complex suggests the presence of both HDEA^+ and HVO_4^{2-} is essential for complex formation. The shape of the stability curve may simply reflect the availability of precursors.^{10a}

The emf studies showed two complexes formed from Tricine and vanadate. The (0,1,1) complex had an overall charge of -1 , and the (1,1,1) complex was neutral. The $\text{p}K_a$ was 3.0. The ^{51}V NMR chemical shift for the (0,1,1) complex did not vary significantly with pH; however, the vanadate dimer showed only small changes in the chemical shift when $\text{HV}_2\text{O}_7^{3-}$ deprotonated to $\text{V}_2\text{O}_7^{4-}$.^{12d,13,24} ^1H and ^{13}C NMR spectra suggest that one carboxylate group, one amine group, and one hydroxyl group are directly attached to the vanadium in the (0,1,1) complex.

A 2D ^{13}C EXSY experiment was used to determine intermolecular microscopic exchange rate constants between Tricine and

the V–Tricine (0,1,1) complex. The microscopic rates were found to be 5.3 and 5.2 s^{-1} at 25°C corresponding to a second-order rate constant of $0.76 \times 10^4 \text{ M}^{-1} \text{ s}^{-1}$ at 25°C . The intermolecular exchange rate constant represents a composite of reactions between the tridentate ligand and vanadate. The calculated second-order rate constant for this reaction corresponded with the previously determined second-order rate constants for EDTA, alizarin, and Na,K–ATPase.^{20,30} These combined observations suggest that the mechanism of the complex formation is a dissociative mechanism governed by loss of a hydroxo or aqua ligand. Since these complexes contain mono, di, tri, tetra, and polydentate ligands, the rate-limiting loss of the hydroxo or aqua ligand should be a common step for all these complexes. Such a step presumably occurs early in the reaction path, possibly before the ligands are in contact with the vanadium. Specifically, the rate-limiting loss of the first hydroxo or aqua ligand would yield second-order rate constants that would be similar for complex formation with such a variety of different ligands. The work presented here, combined with previous studies, suggests vanadium(V) complex formation may follow a dissociative mechanism.

At lower temperatures, intramolecular microscopic exchange rates constants were frozen out and determined to be 3.1 s^{-1} at 0°C (normalized to 36 s^{-1} at 25°C). This intramolecular exchange involves the $-\text{CH}_2\text{O}-$ group attached to the vanadium and the two free $-\text{CH}_2\text{OH}$ groups in the complex. The intramolecular rate constant describes a rate faster than complex decomposition or formation. This intramolecular rate constant is a measure for H_2O exchange with the complex.

This work represents an attempt to structurally and kinetically characterize complexes formed in aqueous solution between vanadate and amino acid derived ligands. The few structural studies of vanadium and peptide-like ligands present difficulties when examining the interactions between multidentate ligands (such as proteins) and vanadate. We have studied two simple amino acid derived ligands that form fairly strong complexes with vanadate and determined structural and kinetic information on these complexes. The structural and the kinetic studies of aqueous vanadate complexes described in this work combined with the reports in literature suggest that vanadium(V) complexes may follow a dissociative path. These observations should assist the thinking of those concerned with the mechanisms by which vanadium(V) interacts in biological systems.

Acknowledgment. This work was supported by a Colorado State Career Advancement Grant, NIH (DCC), and by the Swedish Natural Science Research Council (LP). We thank Dr. Christopher D. Rithner for stimulating discussions and valuable suggestions concerning the 2D ^1H and ^{13}C NMR spectroscopy. We thank Dr. Lars-Olof Öhman for discussions concerning the emf measurements and Dr. Kenneth Kustin for discussions concerning the mechanistic interpretations of this work.

Registry No. DEA, 111-42-2; HDEA⁺, 90578-97-5; Tricine⁻, 132376-21-7; Tricine, 5704-04-1; HTricine⁺, 67303-75-7; VO_4^{3-} , 14333-18-7; HVO_4^{2-} , 26450-38-4; H_2VO_4^- , 34786-97-5; $\text{V}_2\text{O}_7^{4-}$, 22466-30-4; $\text{HV}_2\text{O}_7^{3-}$, 64283-47-2; $\text{H}_2\text{V}_2\text{O}_7^{2-}$, 103884-11-3; $\text{V}_4\text{O}_{13}^{6-}$, 78197-79-2; $\text{HV}_4\text{O}_{13}^{5-}$, 78197-80-5; $\text{V}_4\text{O}_{12}^{4-}$, 12379-27-0; $\text{V}_5\text{O}_{15}^{5-}$, 78197-82-7; $\text{V}_{10}\text{O}_{28}^{6-}$, 12397-12-5; $\text{HV}_{10}\text{O}_{28}^{5-}$, 11117-79-6; $\text{H}_2\text{V}_{10}\text{O}_{28}^{4-}$, 11117-82-1; $\text{H}_3\text{V}_{10}\text{O}_{28}^{3-}$, 55127-68-9; VO_2^+ , 18252-79-4.

(33) (a) Fitzgerald, J. J.; Chasteen, N. D. *Biochemistry* **1974**, *13*, 4338–47. (b) Wüthrich, K.; Connick, R. E. *Inorg. Chem.* **1967**, *6*, 583–90.

(34) Kustin, K.; Liu, S.-T.; Nicolini, C.; Toppen, D. L. *J. Am. Chem. Soc.* **1974**, *96*, 7410–5.